A Combinatorial Approach for the Solution Deposition of Thin Films

ACS APPLIED ENGINEERING MATERIALS

pubs.acs.org/acsaenm Article

A Combinatorial Approach for the Solution Deposition of Thin Films

Noy Zakay, Luca Lombardo, Nitzan Maman, Marco Parvis, Leonid Vradman, and Yuval Golan*

Cite This: https://doi.org/10.1021/acsaenm.3c00072 Read Online

ACCESS | Metrics & More | Article Recommendations | Supporting Information

ABSTRACT: Optimization of thin film deposition is often the limiting step in the discovery of new materials and device development. Over the years, high-throughput combinatorial methods were developed for the deposition of thin films from the gas phase. However, very few reports focused on combinatorial thin film deposition from solution. Here, we introduce a combinatorial approach for the deposition of thin films from solution. The flow deposition setup allows for simultaneously studying the effect of two critical parameters, deposition time and deposition temperature, on a single sample. As a proof of concept, we demonstrate the solution deposition of PbS thin films, which resulted in a library of 25 deposition condition combinations on a single GaAs (100) substrate. X-ray diffraction and scanning electron microscopy combined with focused ion beam cross-sectional sample preparation confirmed the formation of high-quality PbS films and showed the morphology evolution as a function of these two deposition parameters. This method can be easily adapted for cost-effective and rapid combinatorial studies of a large variety of solution-deposited thin film materials.

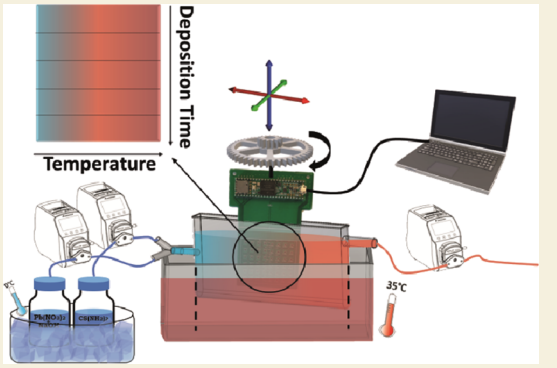

KEYWORDS: *combinatorial materials science, thin films, combinatorial solution deposition, liquid flow deposition, chemical epitaxy*

INTRODUCTION

In recent years, combinatorial technologies have been successfully employed to develop, optimize, and discover new thin film materials in research and industry.[1−8] Combinatorial materials science is a high-efficiency experimental approach to deposit "libraries" of thin films on a single substrate in one experiment and under identical conditions while varying parameters systematically.[8,9] The libraries can include various parameters such as deposition time, temperature, and composition. There are two options for changing parameters during the experiment: discrete steps or continuous gradient.[8,10] The amount of data that can be obtained from a discrete library is determined by the step size, while in a continuous gradient, the amount is limited only by the size of the probe used to characterize the library.[8] Most of the combinatorial research involves gas-phase deposition methods, such as pulsed laser deposition and ion beam sputtering, yielding one parameter (1D) libraries with compositional or substrate temperature gradients.[8,11] These combinatorial methods are efficient, fast, cost-effective, and tremendously time-saving for the research and the researcher. Preparation of a 2D library of thin film samples with a substrate temperature gradient applied in perpendicular to a composition or film thickness gradient on a single substrate further illustrates both the time and expense saved by a combinatorial approach.[7,8,11] Furthermore, with an increased database, it is possible to analyze the results using artificial intelligence methods and gather additional essential information that could not be extracted from individual experiments.[12]

Solution-based deposition of high-quality thin films, including chemical bath deposition (CD),[13−16] was proven to be inexpensive, straightforward, and simple. Furthermore, CD facilitates efficient control over thin film properties.[14,15,17] For example, the thin films of PbS, an important semiconductor with optoelectronic properties applicable for infrared detection and solar cells,[18−21] can be grown on GaAs with unprecedented quality[22] and transformed from nanocrystalline to monocrystalline by controlling growth parameters in CD.[23] However, the main drawback of CD is the depletion of reactant concentrations, giving rise to spatial non-uniformities and limiting the maximum achievable film thickness.[14,24,25] Liquid flow deposition (LFD) is a variation of CD with improved performance[26−28] because a constant solution composition is kept during the entire deposition process by replenished reactants continuously flowing past the reactor and substrate. However, the research and optimization of thin film deposition, CD and LFD, require many experiments demanding resources and time, and resulting in

Received: February 22, 2023
Accepted: April 12, 2023

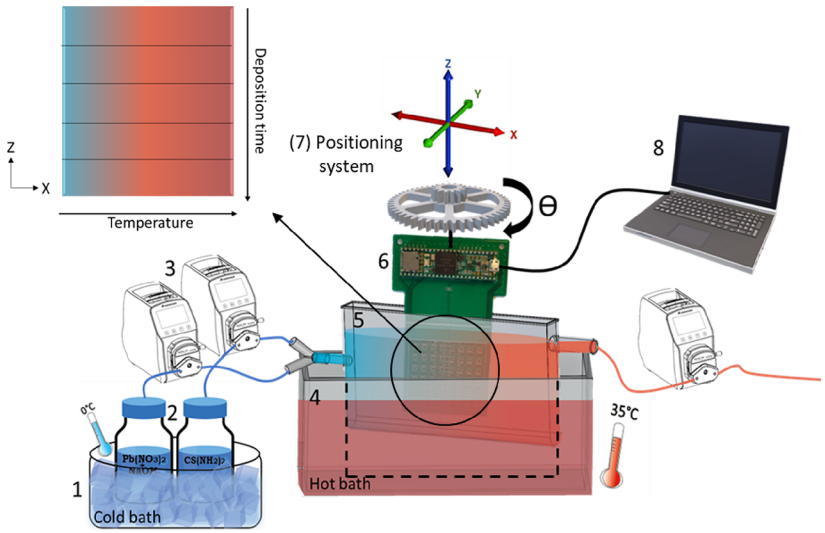

Figure 1. Experimental 2D-CLFD setup including the (1) cold bath, (2) stock solutions, (3) peristaltic pumps, (4) hot bath, (5) flow reactor, (6) PCB holder with GaAs substrate on one side and sensor matrix on the other side (see detailed view in Figure 2), and (7 and 8) computer-controlled positioning system. The reactor was fully immersed in the hot bath during the entire experiment, as indicated by the black dashed lines, and is shown in the illustration to be raised above the hot bath to better visualize the experimental setup. Inset: schematic illustration of the experimental conditions showing the discrete deposition time steps in the *z*-direction vs the temperature gradient along the *x*-direction. Blue denotes cold solution temperature, and red denotes hot solution temperature.

large quantities of wasted solution and substrate. These disadvantages can be overcome by combinatorial solution deposition.

While the combinatorial deposition of thin films is widely focused on the gas-phase methods,[8,11,29−31] there are only few reports on combinatorial solution-based deposition.[32−34] In these reports, a dip coater was used to vary the deposition time by drawing the substrate from solution during CD accompanied by reactant concertation depletion.[32,33] As we reported recently, the liquid flow reactor allowed for constant deposition conditions in combinatorial LFD (CLFD).[34] However, all combinatorial solution-based deposition works were limited to varying one parameter, deposition time, thus producing a 1D combinatorial library. Thus, the deposition of a 2D library of thin films, cost-effectively applied in gas phase methods, was never reported in solution-based deposition systems.

In this research, we have designed and demonstrated, for the first time, a CLFD approach for obtaining a 2D library of thin films (2D-CLFD), covering the temperature−deposition time parameter space on a single substrate. The discrete domains of the deposition times were achieved by drawing up the substrate, while a horizontal temperature gradient was created by feeding cold solutions into an open-top heated flow reactor. As a proof of concept, this approach was illustrated by the deposition of PbS thin films on GaAs(100), widely researched in bath and flow reactors.[17,21,23,24,34,35] The obtained 2D library consisted of PbS thin films with morphologies ranging from nanocrystalline to monocrystalline and thickness exceeding 3.5 μm, demonstrating the validity and potential universality of the 2D-CLFD approach.

EXPERIMENTAL DETAILS

As was elaborated in the Introduction, this work aimed in designing a combinatorial approach for solution deposition of a 2D library of thin films to map the temperature and deposition time parameter space on a single substrate in one experiment. The general design concept of the constructed 2D-CLFD system (Figure 1) was to create a temperature gradient in a flow direction (x) by feeding cold solutions into a heated reactor while minimizing the temperature gradient in a vertical (z) direction (see inset in Figure 1). Thus, the stepwise drawing of the substrate from the reactor will create thin film bands with increasing thickness, grown for increasing deposition time periods under a similar temperature gradient.

To achieve a significant temperature gradient in the flow direction (x) and allow to draw the substrate up (z-direction) to create the steps of deposition time, a long (150 mm), narrow (15 mm), and deep (80 mm) open-top reactor was designed (Figure 1 and Figure S1). The reactor was made of quartz and equipped with inlet and outlet tubes at heights of 44 and 66 mm, respectively. The outlet tube height dictated the liquid level in the reactor so that the total volume of the solution in the reactor was 150 mL. The total flow rate of the source solutions was 60 mL/min, resulting in an average residence time (ratio of the reactor volume and the flow rate) of 2.5 min. The reactor volume as well as all the other relevant deposition conditions (concentrations, temperature range, and flow rate) were chosen based on our previous works, dealing with deposition of PbS thin films using LFD[24] and CLFD.[34] First, in this way, the performance of the new 2D-CLFD system could be directly compared with the previously validated flow deposition systems. Second, it allowed assurance that due to the very short residence time, the conversion of the reactants was very low as well, yielding virtually no concentration gradient in the reactor. This, together with the constant feed of the source solutions, maintained steady-state and uniform precursor concentration in the reactor throughout the deposition experiments.

The lead nitrate and thiourea solutions (2) were kept in 2 L Pyrex bottles at a 0 °C cold bath (1) during the experiment. The solutions were fed using two peristaltic pumps (3) through silicone tubes connected to a Y-connector, where they were mixed right before entering the reactor. Another peristaltic pump, connected to the outlet tube, pumped the spent solution out, ensuring a constant liquid level in the reactor.

The reactor was immersed in the hot bath (4) where a temperature of 35 °C was maintained throughout the experiment. The hot bath and cold solution temperatures were chosen to aim at a deposition temperature range of 20−30 °C, which is optimal for PbS thin film growth.[23,24,34] We note that the reactor conditions can be tuned in a wide range of temperatures (0−90 °C) for larger gradients or different temperature ranges for the deposition of other thin film materials. The reactor immersion depth was 76 mm, leaving its top 4 mm above the

https://doi.org/10.1021/acsaenm.3c00072
ACS Appl. Eng. Mater. XXXX, XXX, XXX−XXX

hot water level in the bath. Since the solution level in the reactor was 66 mm, the entire solution in the reactor was immersed 10 mm below the hot water level in the bath during the entire experiment. The immersed reactor position is shown schematically by the dashed lines (Figure 1), while it appears above the hot bath to clarify the setup presentation.

The positioning system (7), composed of linear motors and multi-axis stages with a repeatability of better than 0.1 mm, allowed for controlled movement in the *x*-, *y*-, *z*-, and θ-directions, serving a twofold purpose. First, it was programmed to fully immerse the assembly of a temperature sensor matrix with the GaAs(100) substrate affixed on the back side of the matrix (6) and draw the sample vertically at designated time intervals to achieve discrete steps of the deposition times along the *z*-direction. In addition, the system facilitated finding an optimal sample position for achieving a significant temperature gradient along the *x*-direction with a minimal gradient in the *z*-direction and reproducing this position in further experiments.

The temperature sensor matrix (6) was specifically designed for accurately monitoring the temperature gradient developed on the GaAs(100) substrate. The sensor matrix employed 48 digital sensors arranged in six rows and eight columns for a total active area of about 5 cm × 5 cm. The sensors were mounted on a printed circuit board (PCB) designed to easily access and attach the PCB to the positioning system and, at the same time, immerse the substrate in the solution (Figures 1 and 2a). The TMP112A temperature digital

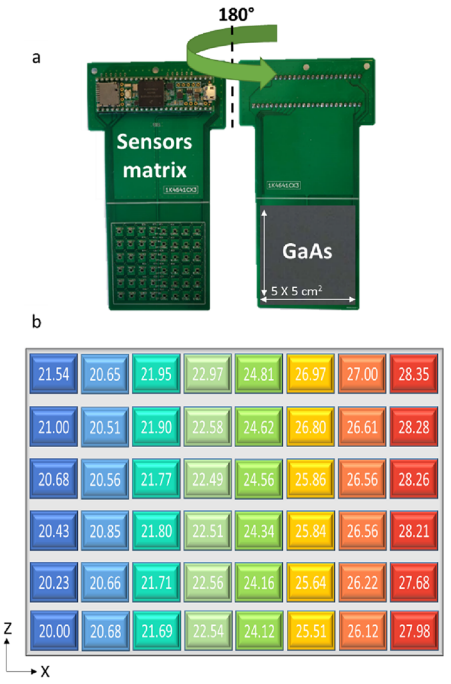

Figure 2. (a) Photograph of the PCB holder. The assembly of the temperature sensor matrix is shown on one side, and the GaAs(100) substrate is shown on the opposite side of the holder. (b) Snapshot of the temperatures measured by the sensors during an experiment.

sensor, manufactured by Texas Instruments, was selected for this application due to its excellent accuracy (typ. 0.25 °C) and low package profile, which allows an overall thickness of less than 1 mm. The layout of the PCB was designed to maximize the heat transfer between the GaAs(100) substrate and the 48 sensor chips in order to improve the sensing accuracy and responsiveness. A Teensy 3.6 controller, mounted on the PCB top, was employed to collect the acquired data and transfer it to a computer, where a dedicated software was used for saving and processing the data. Finally, the entire PCB was coated with a ~80 μm coating of conformal polyurethane (type 1A33, manufactured by HUMISEAL according to the standard IPC/J-STD) to seal the circuits from the deposition solution and avoid degradation in performance during the experiments and upon re-use in additional experiments. Additional details on the temperature sensor design are presented in Figure S2.

The GaAs(100) substrate (5 cm × 5 cm) was attached to the back side of the temperature sensors (Figure 2a) with Bison 6305453 silicone glue and kept for 24 h before the experiment in the desiccator. The very small distance between the sensor matrix and the substrate (<1 mm) allowed the assumption that the measured temperatures are the same as on the surface of the substrate. Figure 2b presents an example of the temperatures measured by the sensors, demonstrating a gradient in the range of 20−28 °C in the *x*-direction and with minimal (1 ± 0.5 °C) gradient in the *z*-direction (see further details in the Results and Discussion section).

Materials

Lead nitrate (Aldrich, analytical 99.99%), sodium hydroxide (Aldrich, ACS ≥98.0%), thiourea (Aldrich, ACS ≥99.0%), acetone (Bio-Lab, technical grade), and 2-propanol (Bio-Lab, 99.8%) were used without further purification. Distilled water (DI water) was obtained using a Millipore Direct Q3. GaAs(100) wafer substrate (±0.1° miscut), undoped and epi-polished on both sides, was purchased from Geo Semiconductor (UK) and manufactured by AXT, Ltd. The substrate was cleaved into a 5 cm × 5 cm rectangle, rinsed with DI water, acetone, and 2-propanol, and dried under a stream of dry nitrogen.

Deposition Procedure

The lead cation stock solution contained 3.2 M NaOH and 60 mM $Pb(NO_3)_2$; the sulfide stock solution contained 102 mM $CS(NH_2)_2$.[24,34] The solutions were kept at 0 °C in the 2 L Pyrex bottles and pumped at a 30 mL/min flow rate, yielding a 60 mL/min total flow rate. The $Pb(NO_3)_2$ and $CS(NH_2)_2$ final concentrations in the feed were 30 and 51 mM, respectively, and the final pH was 14.2. The experiment was carried out for a total of 55 min. The GaAs(100) substrate, initially fully immersed for 15 min, was drawn up every 10 min, yielding a PbS thin film library of five discrete deposition times (15, 25, 35, 45, and 55 min) with a perpendicular continuous temperature gradient along the *x* axis in a range of 20−28 °C.

Characterization Methods

X-ray Diffraction. The orientation and crystallographic phase were studied by XRD using a Panalytical Empyrean powder diffractometer equipped with a PIXcel linear detector and a monochromator on the diffracted beam. The 2θ range of 10−60° was scanned with a step of ~6.25°/min using Cu K_α radiation (λ = 1.5405 Å) source equipped with a position-sensitive X'Celerator detector.

High-Resolution Scanning Electron Microscopy. The surface morphology of the thin films was measured by top-view images using an FEI Verios 460L HRSEM. Acceleration voltages ranged from 3 to 5 kV, and beam currents of 25 pA to 0.2 nA were used. The measurements were carried out without coating the samples.

Focused Ion Beams. Cross-sectional images were taken using a dual-beam FIB/SEM tool (Thermo-Fisher Helios G4 UC). The regions of interest (ROIs) were coated with three different layers. First, 10 nm of electron beam carbon (C) deposition created high contrast between the PbS films and the protecting layer. Above this, 500 nm electron deposition of platinum (Pt) was used to protect the ROI from the ion beam. This layer was followed by ion beam deposition of a 2 μm thick carbon layer for protection and to enable straight cuts and cleaning of the cross section without curtaining effects. After depositing these layers, the ion beam (30 kV Ga) was used to mill near the protected area until the PbS film/GaAs substrate interfaces appeared in the SEM. After milling, the cross section was cleaned with gradually reduced probe currents until a good-quality image was obtained. The film thickness was calculated as an average of five values obtained in each image, and the error bars were calculated from these data sets.

https://doi.org/10.1021/acsaenm.3c00072
ACS Appl. Eng. Mater. XXXX, XXX, XXX−XXX

RESULTS AND DISCUSSION

In order to deposit a 2D library of PbS thin films on a single GaAs(100) substrate, the main design concept of the constructed 2D-CLFD system (Figure 1) was to create a temperature gradient by feeding cold source solutions into the heated reactor. To verify the obtained temperature gradient and the experimental setup performance, preliminary experiments were performed starting with the assembly of a temperature sensor matrix and the GaAs(100) substrate fully immersed in the reactor before the feeding of cold solutions was initiated. All sensors measured the same temperature of 34.5 ± 0.5 °C, close to that set in the hot bath (Figure S3, operation period a), proving the accuracy of the sensors and stability of the heating system. After the feeding of cold solutions was initiated, a temperature gradient began to develop in the flow (x-) direction (Figure S3, operation period b). The leading-edge sensors (blue lines) show much lower temperature than the trailing-edge sensors located downstream, with the highest temperature measured by most downstream sensors (red lines). The steady-state gradient is reached in about 230 s, and thereafter, the gradient remains constant for at least an hour (Figure S3, operation period c, presenting the beginning of the steady-state period), underlining the stability of the heating, cooling, and pumping components of the experimental setup. Furthermore, this transient period is comparable to the average residence time in the reactor of 2.5 min, as expected from the flow reactor. At the steady state, the temperature gradient (also shown in Figure 2b) in the relevant 5 cm × 5 cm part of the reactor is in the range of 20−28 °C in the x-direction, with a minimal (1 ± 0.5 °C) gradient in the z-direction. These results demonstrate that the constructed system fits the main design requirements, providing suitable conditions for the growth of PbS thin film 2D library covering temperature and deposition time parameter space on a single 5 cm × 5 cm GaAs(100) substrate. The deposition experiments, presented below, were carried out under similar conditions, starting by immersing the assembly of sensors with substrates to the reactor after the steady state was reached. The temperatures were verified using the sensors throughout the experiment, while the positioning system was used to reproduce the assembly position as well as draw the substrate upward for varying the deposition time. The GaAs(100) substrate, initially fully immersed for 15 min, was drawn up every 10 min, yielding a PbS thin film library of five discrete deposition times (15, 25, 35, 45, and 55 min) with a perpendicular continuous temperature gradient along the x-axis in a range of 20−28 °C.

Figure 3a shows a photograph of 2D library of PbS thin films deposited on GaAs(100) substrate in one experiment. A change of color from dark gray (characteristic of the GaAs substrate) at low deposition time and temperatures to light gray at longer depositions and higher temperatures indicates the deposition of light gray PbS films with increased thickness. The 2D library was divided into discrete deposition time ″rows″ and averaged temperature ″columns″, yielding 25 deposition time and temperature regions on the substrate selected for characterization by X-ray diffraction (XRD), and high-resolution scanning electron microscopy (HR-SEM) of the cross sections were prepared using a focused ion beam (FIB) in a dual beam tool (Figure 3b). This 2D library replaces the results of 25 conventional CD or LFD experiments, noting that the five temperature columns selected are arbitrary; many additional characterization points along the temperature axis could have been selected considering the continuous temperature gradient in the x-direction.

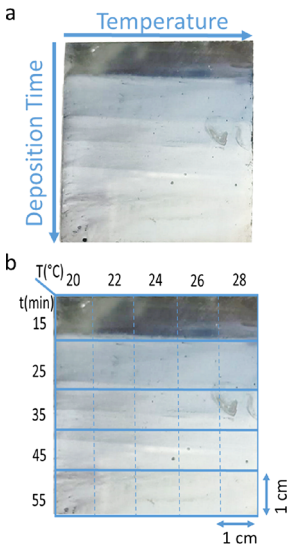

Figure 3. (a) Photograph of a PbS thin film deposited on a GaAs(100) substrate using 2D-CLFD covering a range of deposition times and temperatures. (b) Same image, with an overlaid schematic illustration of the discrete deposition time ″rows″ and virtual temperature ″columns″, yielding 25 deposition time and temperature regions on the substrate that were selected for characterization.

X-ray diffraction results indicated the deposition of a single-phase PbS film with reflections corresponding to rock salt PbS (JCPDS #5-592) in all regions of the 2D library, as presented in Figure S4 for selected regions. At the initial deposition time and low temperature, the films were <111>-oriented (Figure S4a), and a transition to <110>-oriented films was observed at longer depositions and higher temperatures (Figures S4b). These findings indicate how 2D-CLFD improves film deposition optimization and, under favorable conditions, results in a PbS film with a single, well-defined orientation. This is consistent with the HR-SEM results shown below and previously published results on CD,[17,23] LFD,[24] and CLFD[34] of PbS. As mentioned in the Introduction, one of the advantages of the LFD method is larger film thicknesses compared to the CD method, thanks to the constant reactant concentrations. Therefore, during long times and high temperatures, the thickness of the film was considerably high (micrometers thick), and thus, the 220 peak intensity was exceptionally high (over 2 × 10^6 counts). Consequently, the ratio of the 220 to 111 peaks increased rapidly until a state where the 111 peak was negligible compared to 220 was reached. Therefore, a plot of intensity ratios was not relevant here.

Hence, Figure 4 presents a color map with the integrated diffraction intensity for only the 220 Bragg reflections and demonstrates how deposition time and temperature significantly impact the orientation of PbS. As expected, longer deposition times and higher temperatures lead to higher 220 peak intensities due to increased film thickness. This behavior was previously reported in a series of CD experiments.[23] In addition, a similar trend was detected using the CLFD method spanning the effect of deposition time (single parameter combinatorial study).[34] Thus, our 2D-CLFD experiment on a

https://doi.org/10.1021/acsaenm.3c00072
ACS Appl. Eng. Mater. XXXX, XXX, XXX−XXX

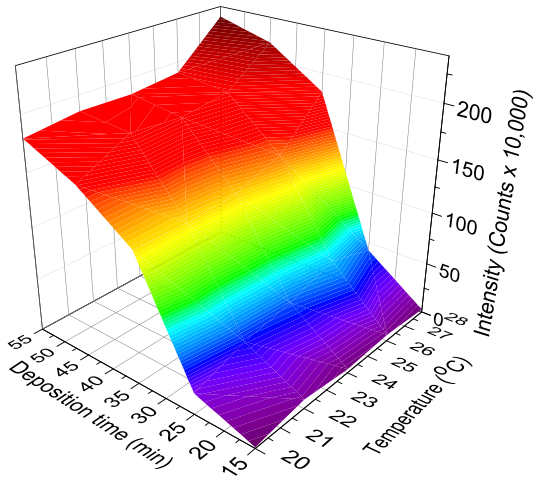

Figure 4. XRD 220 Bragg reflection intensities for PbS thin films deposited on GaAs(100) using 2D-CLFD plotted vs deposition time and temperature.

single substrate replaces at least 25 CD or 5 CLFD experiments.

HR-SEM images of PbS thin films taken from all regions of the 2D library demonstrate topography evolution as a function of deposition time and temperature (Figure 5). Deposition at lower temperatures and short time periods resulted in a nanocrystalline film consisting of round particles with a typical size of ∼125 nm (15 min, 20 °C). An increase in the temperature (left to right in the 15 min row) resulted in an increase in grain size to ∼250 nm and development of the characteristic rectangular topography for <110> out-of-plane orientation (crystallographic axis perpendicular to the substrate surface). The increase in deposition time also causes the evolution of growth orientations from randomly oriented particles at initial deposition times to <110>-oriented crystals (top-to-bottom in the 20 °C column). A longer deposition time (45 min, 20 °C) results in a complete transition to a monocrystalline film with the same orientation. The HR-SEM results are consistent with the XRD findings (Figure S4 and Figure 4), which indicate a transition to <110>-oriented films with increasing deposition time and temperature. This trend is consistent with the nucleation and growth processes typical for solution-based thin film deposition[14] and was reported previously from a series of PbS CD experiments.[23]

Analysis of the crystallographic directions observed on the sample surface is straightforward considering the XRD results and the HR-SEM images. Note that the characterization of the substrate in HR-SEM was also carried out combinatorially since the substrate was placed in one piece in the SEM chamber while maintaining the relative orientation of all 25 deposition condition regions, a unique and important feature demonstrating another inherent advantage of the 2D CLFD method. Due to this unique feature, we were able to detect findings that could not have been obtained from 25 separate samples. For example, Figure 6a,b shows magnified images from two different regions in Figure 5, corresponding to the 25 min/22 °C and 35 min/28 °C deposition conditions. An angle of 35.5° is observed between the elongated rectangular [110] in-plane direction in the $(1\bar{1}1)$ surface (Figure 6a) and the striations along the [111] in-plane direction in the $(1\bar{1}0)$ surface (Figure 6b), in agreement with the XRD data in Figure S4. This phenomenon is common for NaCl systems[17] and was similarly reported by Templeman et al. for PbS thin films on GaAs(111).[36]

The time−temperature superposition is well known and occurs since the deposition rates strongly depend upon the deposition temperature, as proven in previous works.[17,23,24,34] The noteworthy advantage of the 2D CLFD approach is that this superposition is clearly demonstrated in one experiment on a single GaAs(100) substrate analyzing the plan-view HRSEM images (Figure 5) diagonally: from top-left (15 min, 20 °C) to bottom-down (55 min, 28 °C). It shows the transition from nanocrystalline to monocrystalline films. Furthermore, it is known that morphology transitions can often occur through a thermodynamic instability zone. This area would have been very hard to discover without employing a combinatorial deposition approach and subsequent charac-

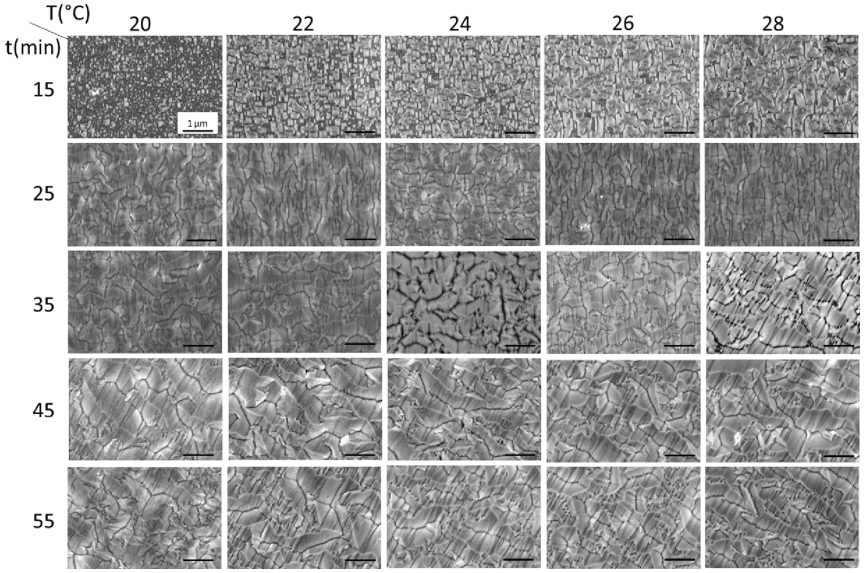

Figure 5. Top-view HRSEM images obtained from the same PbS thin film deposited on a single GaAs(100) substrate using 2D-CLFD. All scale bars correspond to 1 μm.

https://doi.org/10.1021/acsaenm.3c00072
ACS Appl. Eng. Mater. XXXX, XXX, XXX−XXX

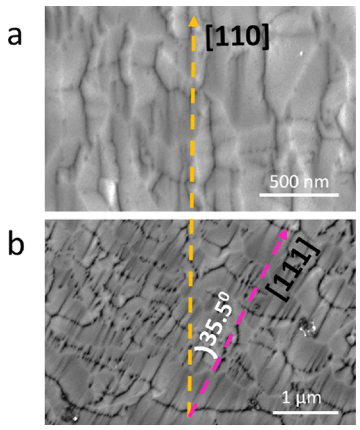

Figure 6. Magnified HR-SEM images of PbS thin films deposited using 2D-CLFD under different deposition parameters: (a) 25 min/22 °C and (b) 35 min/28 °C. The transition from a PbS($1\bar{1}1$)-oriented film with surface striations along the [110] in-plane direction to a PbS($1\bar{1}0$)-oriented film with surface striations along the [111] in-plane direction is clearly seen in agreement with the XRD data in Figure S4. As expected for the cubic structure, the angle between these two in-plane crystallographic directions is 35.5°.

terization. Over time and under different experimental conditions (such as temperature, concentration, pH, etc.), the film morphology and microstructure can vary significantly.[23] Interestingly, Figure 5 shows a region of instability at 35 min and 24 °C, as previously discovered accidentally by Osherov and Golan upon preparation of a series of individual samples.[23]

While these morphological instabilities with a characteristic increased surface roughness have been infrequently reported to date, the 2D-CLFD method allows us to detect these instabilities without difficulty on a single GaAs(100) substrate. It would indeed require many single experiments (e.g., the traditional CD and LFD methods) to detect these instabilities. Thus, the advantage of the new 2D-CLFD method presented in this study is not only in the acceleration of thin-film research and optimization of the deposition parameters but also in the discovery of valuable mechanistic information on morphology evolution during thin film growth.

The prediction of film microstructures based on deposition parameters has been demonstrated by the structural zone model (SZM), first established by Thornton for films deposited using PVD[37] and expanded by Templeman to solution-deposited films.[22] Based on our results, a SZM was constructed and is presented in Figure 7. It is seen that during

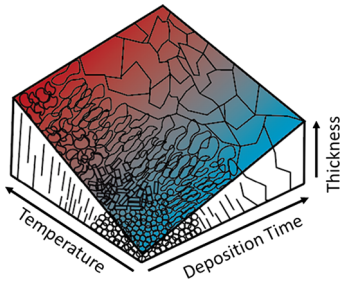

Figure 7. SZM for PbS on GaAs(100) as a function of growth temperature and deposition time. With increasing deposition time and temperature, transformation takes place from a randomly oriented polycrystalline film to a <111>-oriented monocrystalline film.

short deposition times and low temperatures, the film is composed of small clusters. With increasing temperature and deposition time, a transition to nucleation and growth is observed, and upon further increase, monocrystalline growth is dominant.

Cross-sectional images obtained using FIB revealed the formation of high-quality, dense PbS thin film, as demonstrated for the 55 min/28 °C deposition conditions (Figure 8a). The film thickness, obtained from the cross-sectional

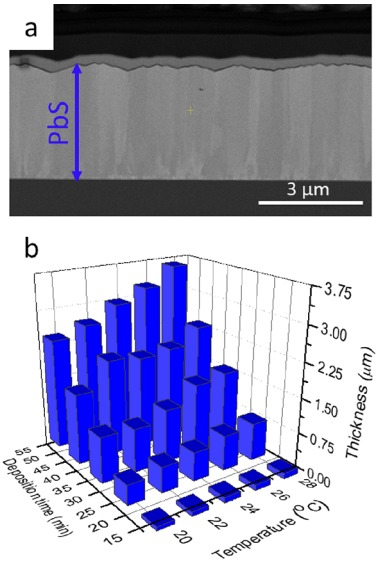

Figure 8. (a) Typical FIB cross-sectional image of a PbS thin film deposited on a GaAs(100) substrate using 2D-CLFD, (55 min, 28 °C). (b) Thickness of PbS thin films obtained from FIB images plotted vs deposition time and temperature.

images of 25 regions, ranges from tens of nm to a few μm and increases with temperature and deposition time (Figure 8b), in agreement with growth kinetics established in our previous studies.[23,24,34] It is noteworthy to mention that the obtained thickness exceeds 3 μm, which is significantly higher than that obtained in CD.[14,23] A few-micrometer thickness was obtained while maintaining adherence to the substrate, which is essential for the practical usage of thin films. These results demonstrate that a single 2D-CLFD experiment provides a complete range of relevant PbS film thicknesses as a function of temperature and deposition time, facilitating the optimization of deposition conditions for a desired thickness required for a given application. As the 2D-CLFD system cost-effectively revealed the morphology evolution of PbS thin films, it is broadly applicable for various fields of thin film research such as the study of phase control as a function of deposition time and temperature, discovery of new materials and compositions, control of thin film properties, and more.

CONCLUSIONS

A new generic method for carrying out the combinatorial deposition of thin films from solution was demonstrated. The method resulted in a 2D library that simultaneously investigated a large number of deposition time and temperature conditions on a single sample under otherwise identical conditions, thus eliminating many possible experimental errors. As a proof of concept for this method, we demonstrated the combinatorial deposition of PbS on GaAs(100), a widely

https://doi.org/10.1021/acsaenm.3c00072
ACS Appl. Eng. Mater. XXXX, XXX, XXX−XXX

studied system. The films obtained were found to be on-par with previous films obtained from batch (CD) and flow (LFD) reactors. In addition, we detected structural instabilities in the morphology evolution that is unlikely to be discovered in a series of conventional, discrete experiments (e.g., CD and LFD). The method will be used to investigate many other thin film materials, resulting in fast, efficient, and cost-effective research and development of thin film materials and properties.

■ ASSOCIATED CONTENT

Supporting Information

The Supporting Information is available free of charge at https://pubs.acs.org/doi/10.1021/acsaenm.3c00072.

Schematic illustration of the reactor for combinatorial deposition, schematic illustration of the temperature sensor matrix, temperature vs time as measured by the sensors, and XRD characterization (PDF)

■ AUTHOR INFORMATION

Corresponding Author

Yuval Golan − *Department of Materials Engineering, Ben Gurion University of the Negev, Beer-Sheva 8410501, Israel; The Ilse Katz Institute for Nanoscale Science and Technology, Ben-Gurion University of the Negev, Beer-Sheva 8410501, Israel;* orcid.org/0000-0003-1369-0285; Email: ygolan@bgu.ac.il

Authors

Noy Zakay − *Department of Materials Engineering, Ben Gurion University of the Negev, Beer-Sheva 8410501, Israel; The Ilse Katz Institute for Nanoscale Science and Technology, Ben-Gurion University of the Negev, Beer-Sheva 8410501, Israel;* orcid.org/0000-0001-8719-2591

Luca Lombardo − *Department of Electronics and Telecommunications, Politecnico di Torino, 10129 Turin, Italy;* orcid.org/0000-0002-6050-111X

Nitzan Maman − *The Ilse Katz Institute for Nanoscale Science and Technology, Ben-Gurion University of the Negev, Beer-Sheva 8410501, Israel*

Marco Parvis − *Department of Electronics and Telecommunications, Politecnico di Torino, 10129 Turin, Italy*

Leonid Vradman − *Department of Chemical Engineering, Ben-Gurion University of the Negev, Beer-Sheva 8410501, Israel; Department of Chemistry, Nuclear Research Centre Negev, Beer-Sheva 84190, Israel;* orcid.org/0000-0002-5099-1952

Complete contact information is available at: https://pubs.acs.org/10.1021/acsaenm.3c00072

Author Contributions

The manuscript was written through contributions of all authors. All authors have given approval to the final version of the manuscript.

Notes

The authors declare no competing financial interest.

■ ACKNOWLEDGMENTS

This work was supported by Israel Science Foundation grant #1760/18.

■ REFERENCES

(1) Mao, S. S.; Burrows, P. E. Combinatorial screening of thin film materials: An overview. *J. Materiomics* **2015**, *1*, 85−91.

(2) Amis, E. J.; Xiang, X.-D.; Zhao, J.-C. Combinatorial materials science: What's new since Edison? *MRS Bull.* **2002**, *27*, 295−300.

(3) Porter, M. D., *Combinatorial Materials Science*; John Wiley & Sons, 2007.

(4) Benayad, A.; Diddens, D.; Heuer, A.; Krishnamoorthy, A. N.; Maiti, M.; Cras, F. L.; Legallais, M.; Rahmanian, F.; Shin, Y.; Stein, H.; Winter, M.; Wölke, C.; Yan, P.; Cekic-Laskovic, I. High-throughput experimentation and computational freeway lanes for accelerated battery electrolyte and interface development research. *Adv. Energy Mater.* **2022**, *12*, 2102678.

(5) Takeuchi, I.; Lauterbach, J.; Fasolka, M. J. Combinatorial materials synthesis. *Mater. Today* **2005**, *8*, 18−26.

(6) Maier, W. F.; Stöwe, K.; Sieg, S. Combinatorial and high-throughput materials science. *Angew. Chem., Int. Ed.* **2007**, *46*, 6016−6067.

(7) Siol, S.; Dhakal, T. P.; Gudavalli, G. S.; Rajbhandari, P. P.; DeHart, C.; Baranowski, L. L.; Zakutayev, A. Combinatorial reactive sputtering of In2S3 as an alternative contact layer for thin film solar cells. *ACS Appl. Mater. Interfaces* **2016**, *8*, 14004−14011.

(8) McGinn, P. J. Thin-Film Processing Routes for Combinatorial Materials Investigations—A Review. *ACS Comb. Sci.* **2019**, *21*, 501−515.

(9) Jandeleit, B.; Schaefer, D. J.; Powers, T. S.; Turner, H. W.; Weinberg, W. H. Combinatorial materials science and catalysis. *Angew. Chem., Int. Ed.* **1999**, *38*, 2494−2532.

(10) Rajan, K. Combinatorial materials sciences: Experimental strategies for accelerated knowledge discovery. *Annu. Rev. Mater. Res.* **2008**, *38*, 299−322.

(11) Talley, K. R.; Sherbondy, R.; Zakutayev, A.; Brennecka, G. L. Review of high-throughput approaches to search for piezoelectric nitrides. *J. Vac. Sci. Technol., A* **2019**, *37*, No. 060803.

(12) Ziatdinov, M. A.; Liu, Y.; Morozovska, A. N.; Eliseev, E. A.; Zhang, X.; Takeuchi, I.; Kalinin, S. V. Hypothesis learning in automated experiment: application to combinatorial materials libraries. *Adv. Mater.* **2022**, *34*, 2201345.

(13) Meldrum, F. C.; Flath, J.; Knoll, W. Chemical deposition of PbS on a series of ω-functionalised self-assembled monolayers. *J. Mater. Chem.* **1999**, *9*, 711−723.

(14) Hodes, G., *Chemical solution deposition of semiconductor films*. CRC press: 2002, DOI: 10.1201/9780203909096.

(15) Friedman, O.; Upcher, A.; Templeman, T.; Ezersky, V.; Golan, Y. Chemical epitaxy of CdS on GaAs. *J. Mater. Chem. C* **2017**, *5*, 1660−1667.

(16) Templeman, T.; Biton, M.; Safrani, T.; Shandalov, M.; Yahel, E.; Golan, Y. Chemically deposited PbSe thin films: factors deterring reproducibility in the early stages of growth. *CrystEngComm* **2014**, *16*, 10553−10559.

(17) Osherov, A.; Ezersky, V.; Golan, Y. The role of solution composition in chemical bath deposition of epitaxial thin films of PbS on GaAs (100). *J. Cryst. Growth* **2007**, *308*, 334−339.

(18) Biancardo, M.; Krebs, F. C. Microstructured extremely thin absorber solar cells. *Sol. Energy Mater. Sol. Cells* **2007**, *91*, 1755−1762.

(19) Li, H.; Zhitomirsky, D.; Grossman, J. C. Tunable and energetically robust PbS nanoplatelets for optoelectronic applications. *Chem. Mater.* **2016**, *28*, 1888−1896.

(20) Osherov, A.; Golan, Y. Chemical epitaxy of semiconductor thin films. *MRS Bull.* **2010**, *35*, 790−796.

(21) Bernabucci, F.; Margaritondo, G.; Migliorato, P.; Perfetti, P. Near-IR detection by PbS- GaAs heterojunctions. *Phys. Status Solidi A* **1973**, *15*, 621−627.

(22) Templeman, T.; Sengupta, S.; Maman, N.; Bar-Or, E.; Shandalov, M.; Ezersky, V.; Yahel, E.; Sarusi, G.; Visoly-Fisher, I.; Golan, Y. Oriented attachment: a path to columnar morphology in chemical bath deposited PbSe thin films. *Cryst. Growth Des.* **2018**, *18*, 1227−1235.

(23) Osherov, A.; Ezersky, V.; Golan, Y. Microstructure and morphology evolution in chemically deposited semiconductor films: 4. From isolated nanoparticles to monocrystalline PbS thin films on GaAs (100) substrates. *Eur. Phys. J. Appl. Phys.* **2007**, *37*, 39−47.
(24) Murza, V.; Friedman, O.; Vradman, L.; Golan, Y. Liquid flow deposition of PbS films on GaAs (100). *CrystEngComm* **2018**, *20*, 3765−3771.
(25) McPeak, K. M.; Baxter, J. B. Microreactor for high-yield chemical bath deposition of semiconductor nanowires: ZnO nanowire case study. *Ind. Eng. Chem. Res.* **2009**, *48*, 5954−5961.
(26) Le, D. T.; Jeon, C. J.; Lee, K. W.; Jeong, Y. H.; Yun, J. S.; Yoon, D. H.; Cho, J. H. Liquid flow deposited spinel $(Ni, Mn)_3O_4$ thin films for microbolometer applications. *Appl. Surf. Sci.* **2015**, *330*, 366−373.
(27) Goto, Y.; Tamaura, Y.; Gomi, M.; Abe, M. Ferrite Plating by Means of Thin Film of Reaction Solution;″ Thin Liquid-Film Method″. *IEEE Transl. J. Magn. Jpn.* **1987**, *2*, 235−236.
(28) Goto, Y.; Tamaura, Y.; Abe, M.; Gomi, M. Improvement in Deposition Rate and Quality of Films Prepared by″ Thin Liquid-Film″ Ferrite Plating Method. *IEEE Transl. J. Magn. Jpn.* **1988**, *3*, 159−165.
(29) Aimon, N. M.; Hun Kim, D.; Kyoon Choi, H.; Ross, C. A. Deposition of epitaxial $BiFeO_3/CoFe_2O_4$ nanocomposites on (001) $SrTiO_3$ by combinatorial pulsed laser deposition. *Appl. Phys. Lett.* **2012**, *100*, No. 092901.
(30) Matsumoto, Y.; Murakami, M.; Jin, Z.; Ohtomo, A.; Lippmaa, M.; Kawasaki, M.; Koinuma, H. Combinatorial laser molecular beam epitaxy (MBE) growth of Mg−Zn−O alloy for band gap engineering. *Jpn. J. Appl. Phys.* **1999**, *38*, L603.
(31) Chen, W.; Liu, Q.; Liu, Q.; Zhu, L.; Wang, L. A combinatorial study of the corrosion and mechanical properties of Zn−Al material library fabricated by ion beam sputtering. *J. Alloys Compd.* **2008**, *459*, 261−266.
(32) Mokurala, K.; Baranowski, L. L.; de Souza Lucas, F. W.; Siol, S.; van Hest, M. F. A. M.; Mallick, S.; Bhargava, P.; Zakutayev, A. Combinatorial chemical bath deposition of CdS contacts for chalcogenide photovoltaics. *ACS Comb. Sci.* **2016**, *18*, 583−589.
(33) Yan, Z.; Zhang, X.; Li, G.; Cui, Y.; Jiang, Z.; Liu, W.; Peng, Z.; Xiang, Y. High-throughput combinatorial chemical bath deposition: The case of doping Cu (In, Ga) Se film with antimony. *Appl. Surf. Sci.* **2018**, *427*, 1235−1241.
(34) Zakay, N.; Friedman, O.; Vradman, L.; Golan, Y. Combinatorial Liquid Flow Deposition of PbS Semiconductor Thin Films. *Ind. Eng. Chem. Res.* **2021**, *60*, 15593−15599.
(35) Osherov, A.; Golan, Y. Chemical solution deposited PbS thin films on Si (100). *Phys. Status Solidi C* **2008**, *5*, 3431−3436.
(36) Templeman, T.; Perez, M.; Friedman, O.; Abutbul, R. E.; Shandalov, M.; Ezersky, V.; Konovalov, O.; Golan, Y. Layer-by-layer growth in solution deposition of monocrystalline lead sulfide thin films on GaAs (111). *Mater. Chem. Front.* **2019**, *3*, 1538−1544.
(37) Thornton, J. A. Influence of apparatus geometry and deposition conditions on the structure and topography of thick sputtered coatings. *J. Vac. Sci. Technol.* **1974**, *11*, 666−670.

https://doi.org/10.1021/acsaenm.3c00072
ACS Appl. Eng. Mater. XXXX, XXX, XXX−XXX